Electronic structure, x-ray photoemission spectra, and transport properties of Fe_3C (cementite)

J. Häglund and G. Grimvall
Department of Theoretical Physics, The Royal Institute of Technology, S-100 44 Stockholm, Sweden

T. Jarlborg
Département de Physique de la Matière Condensée, Université de Genève, CH-1211 Genève, Switzerland
(Received 28 January 1991)

We have performed a detailed linear-muffin-tin-orbitals calculation of the electronic structure of Fe_3C (cementite). The orthorhombic unit cell contains 16 atoms, with 4 Fe atoms taking type-1 positions which are not equivalent to the type-2 positions of the other 8 Fe atoms. The calculated moments in the ferromagnetic state are $\mu = 1.98\mu_B$ on the Fe(1) sites, $\mu = 1.74\mu_B$ on the Fe(2) sites, and $\mu = -0.06\mu_B$ on the carbon sites, in excellent agreement with experiment. The hyperfine fields in Fe_3C have been calculated from the spin densities at the center of each atom. We obtain $B = 26.9$ T on the Fe(1) sites, $B = 25.7$ T on the Fe(2) sites, and $B = 0.23$ T on the carbon sites. The calculated electron states are in qualitative agreement with x-ray photoemission spectroscopic data. The electron-phonon coupling parameter estimated from our calculations is $\lambda = 0.77$. This gives an electronic heat capacity close to the experimental one. Experimental data on the electrical resistivity are uncertain and larger than our estimated value $\rho = 47$ $\mu\Omega$cm at 300 K. The calculated cohesive energy per atom $E_{\rm coh} = 615$ mRy is to be compared with the estimate $E_{\rm coh} = 370$ mRy based on experimental information.

I. INTRODUCTION

Pure iron transforms from a low-temperature bcc structure to an fcc structure at 1184 K. The close-packed fcc phase has a high solubility of carbon while the solubility in the bcc phase is low. When iron with carbon in solid solution is cooled from high temperatures, cementite (Fe_3C) precipitates. The morphology of these precipitations is of decisive importance for the mechanical properties of iron alloys. Therefore, cementite has been studied in much detail, when considered as a structural component of steel. Contrasting this, little is known, experimentally and theoretically, about the physical properties of pure cementite. One reason is the experimental difficulty to prepare specimens of cementite. Often the properties of cementite have been deduced from measurements on two-phase systems with cementite in an iron matrix.

Cementite has an orthorhombic structure, with 16 atoms per unit cell. It is a ferromagnetic metal. The magnetic moment is well known experimentally,[1,2] but only as an average over the iron positions. There are relatively few spectroscopic investigations, and the only complete x-ray photoemission spectroscopic (XPS) spectrum of the valence band[3] refers to a temperature well above the Curie temperature. The electrical resistivity has been reported in several works[4–6] but the results are widely differing.

Considering the technological importance of cementite, and the incompleteness and uncertainty in the experimental data, there is strong motivation for a detailed *ab initio* calculation of the electron band structure and properties derived from that. We know of only one previous band-structure calculation for cementite,[7] which, however, is not accurate or detailed enough for our purpose.

In this work, we present theoretical results for a number of physical properties of Fe_3C, related to the electronic structure. Our analysis is based on a spin-polarized, semirelativistic band-structure calculation using the linear-muffin-tin-orbitals (LMTO) method. The outline of the paper is as follows. In Sec. II we summarize what structural and computational parameters that were used in the LMTO calculation. The electronic energy bands and density-of-states curves are presented in Sec. III. In this section we also compare our magnetic moments, hyperfine fields, and cohesive energies with experimental results. An estimate of the electron-phonon coupling constant is also determined. In Sec. IV we discuss spectroscopic results and a theoretical XPS intensity, calculated by us, is compared with an experimental curve. Contributions from different angular momentum transitions are separated and the energy variations of the corresponding matrix elements are studied. Before concluding, we discuss the electrical resistivity of cementite in Sec. V. The electron-phonon coupling constant is used to get a theoretical estimate of the resistivity. This is found to be considerably lower than most experimentally determined values. A possible explanation is that the experiments refer to nonideal Fe_3C crystals.

II. COMPUTATIONAL AND STRUCTURAL PARAMETERS

The band-structure calculation was performed using the semirelativistic LMTO method described

elsewhere.[8,9] The local-density approximation with the Gunnarsson-Lundqvist parametrization was adopted to get a self-consistent potential from the charge density. The energy spectrum was calculated for a 64-**k**-point mesh in an irreducible wedge of the Brillouin zone. The basis functions were chosen to include s, p, and d states for the iron atoms and s and p states for the carbon atoms. The atomic spheres were made larger for the iron atoms than for the carbon atoms by setting the Wigner-Seitz (WS) radii equal to $R_{\mathrm{WS}}^{\mathrm{Fe}} = 0.299a$ and $R_{\mathrm{WS}}^{\mathrm{C}} = 0.272a$, where a is the lattice parameter.

Fe_3C crystallizes in an orthorhombic structure with the space group V_h^{16} (D_{2h}^{16};$Pbnm$).[10] The unit cell contains 4 carbon atoms, 4 iron atoms of type 1 and 8 iron atoms of type 2, i.e., a total of 16 atoms. Fe(1) and Fe(2) are two stoichiometrically different iron sites. Atomic positions and lattice constants are listed in Table I.

III. BAND-STRUCTURE RESULTS

The majority and minority bands of Fe_3C are plotted in Figs. 1 and 2. The corresponding density of states (DOS) curves are shown in Fig. 3. The general features of the energy spectrum are the same as for the simple NaCl-structure carbide FeC.[11] The lowest-lying bands are carbon s bands which range from -0.44 to -0.29 Ry. A band gap up to 0.03 Ry separates these bands from a region dominated by hybridized carbon p states and iron d states. The Fermi level, at 0.66 Ry, falls in a dense part of the energy spectrum where the only important contribution to the density of states comes from iron d states. From the projections in Fig. 3 it is seen that iron s and p states only give small DOS contributions.

TABLE I. Crystal data of cementite. a_0, b_0, and c_0 are the lengths in Å of the unit vectors of the orthorhombic unit cell. The atomic positions are all in units of a_0.

a_0	4.523		
b_0	5.089		
c_0	6.743		
Fe(1)	0.833	0.045	0.373
	0.167	1.080	1.118
	0.667	0.608	0.373
	0.333	0.518	1.118
Fe(2)	0.333	0.197	0.097
	0.667	0.928	1.394
	0.167	0.759	0.648
	0.833	0.366	0.842
	0.667	0.928	0.842
	0.333	0.197	0.648
	0.833	0.366	1.394
	0.167	0.759	0.097
C	0.430	0.979	0.373
	0.570	0.146	1.118
	0.070	0.416	0.373
	0.930	0.709	1.118

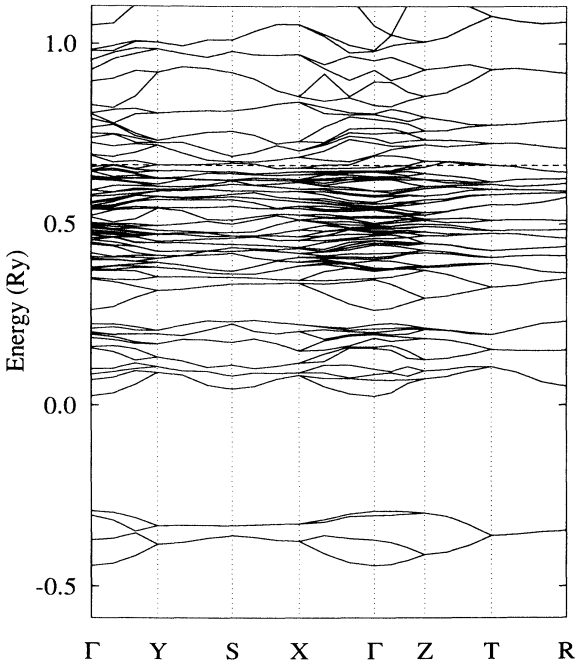

FIG. 1. Majority bands of Fe_3C.

Fe_3C is known to be ferromagnetic. Its magnetic moments do not seem to have been theoretically calculated before. We obtain $\mu = 1.98\mu_B$ on the Fe(1) sites, $\mu = 1.74\mu_B$ on the Fe(2) sites, and $\mu = -0.06\mu_B$ on the carbon sites. The relatively large difference be-

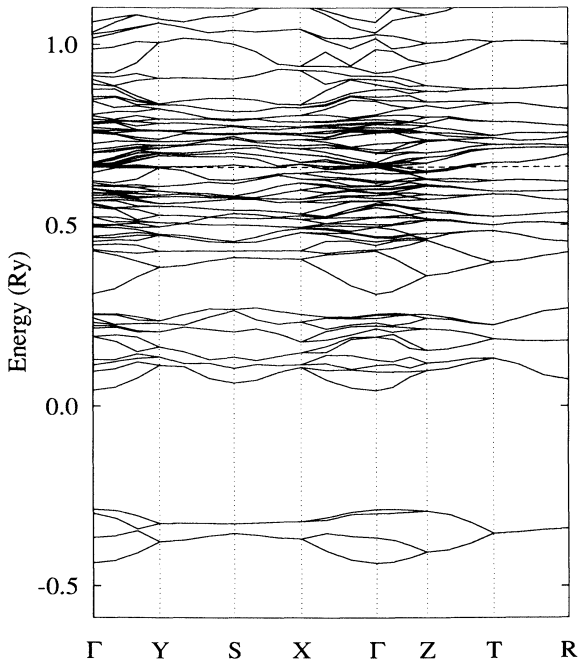

FIG. 2. Minority bands of Fe_3C.

tween the magnetic moments of the two iron sites is similar to that found in the related compound Fe_3B.[12] Experimental information is only available for the average magnetic moment ($\overline{\mu}$) of iron atoms in Fe_3C. Reference 1 gives $\overline{\mu}_{Fe} = 1.72\mu_B - 1.78\mu_B$ while Shabanova and Trapeznikov[2] quote the measured value $\overline{\mu}_{Fe} = 1.78\mu_B$. Averaging over our theoretically determined iron moments gives $\overline{\mu}_{Fe} = 1.82\mu_B$, thus slightly higher than the experimental values. This deviation is expected since the local-density approximation is known to overestimate the magnetic moments in ferromagnetic metals. (See Table II.)

The hyperfine fields in Fe_3C have been calculated from the spin densities at the center of each atom. We obtain $B = 26.9$ T on the Fe(1) sites, $B = 25.7$ T on the Fe(2) sites, and $B = 0.23$ T on the carbon sites. The calculated hyperfine fields on the iron atoms of Fe_3C compare favorably with the experimental values $B = 20.7$ and 20.5 T for Fe(1) and Fe(2), respectively.[13]

The cohesive properties of 3*d*-transition-metal carbides have been studied both experimentally and theoretically.[14] However, *ab initio* results are available only for NaCl-structure carbides in the series.[11] It is therefore of considerable interest to calculate the cohesive energies of the more complex transition-metal carbides. For Fe_3C, we find a total electronic energy of $E_{tot} = -30\,799.3 \pm 0.1$ Ry per unit cell. This value can be used to derive the cohesive energy per atom through the relation

$$E_{coh} = \left(\frac{1}{16}\right)\left(E_{tot} - \sum E_A\right), \tag{1}$$

where the total atomic energies E_A are to be summed over all 16 atoms of the unit cell. Using previously determined[11] atomic energies, we obtain $E_{coh} = 615$ mRy/atom$=8.07 \times 10^5$ J/mol. This value can be compared with $E_{coh} = 370 \pm 5$ mRy/atom, an estimate from a recent evaluation of experimental information.[15]

The electron-phonon coupling parameter (λ) can, due to the large mass difference between the iron and carbon atoms, be estimated as[16]

$$\lambda = \frac{\eta_{Fe}}{M_{Fe}\langle\omega_{Fe}^2\rangle} + \frac{\eta_C}{M_C\langle\omega_C^2\rangle}. \tag{2}$$

The numerators, η_{Fe} and η_C, depend on the electronic structure and can be expressed in LMTO results. For each atom one can write[17,18]

$$\eta = \frac{1}{N}\sum_l \frac{(l+1)N_l N_{l+1}(P_{l+1}-P_l)^2 R_l^2 R_{l+1}^2}{(2l+1)(2l+3)(j_l P_l - n_l)^2 (j_{l+1}P_{l+1} - n_{l+1})^2}, \tag{3}$$

$$P_l = (2l+1)\frac{D_l + l + 1}{D_l - l}. \tag{4}$$

D_l is the logarithmic derivative, R_l is the radial part of the wave function, and j_l and n_l are the amplitudes of the Bessel and Neumann functions, all evaluated at the WS radius. The denominators in Eq. (2) include atomic masses (M_{Fe} and M_C) and averages over the phonon frequencies at each site:

$$\langle\omega^2\rangle = \frac{\int \omega\alpha^2 F(\omega)\, d\omega}{\int [\alpha^2 F(\omega)/\omega]\, d\omega}, \tag{5}$$

where $\alpha^2 F(\omega)$ is the electron-phonon coupling function.[19] In the diatomic case,[20] a widely used approximation is to write $\langle\omega_M^2\rangle \approx \langle\omega_{ac}^2\rangle$ and $\langle\omega_C^2\rangle \approx \langle\omega_{op}^2\rangle$ since the acoustic vibrations mostly can be ascribed to the metal sites while the lighter nonmetal carbon atoms

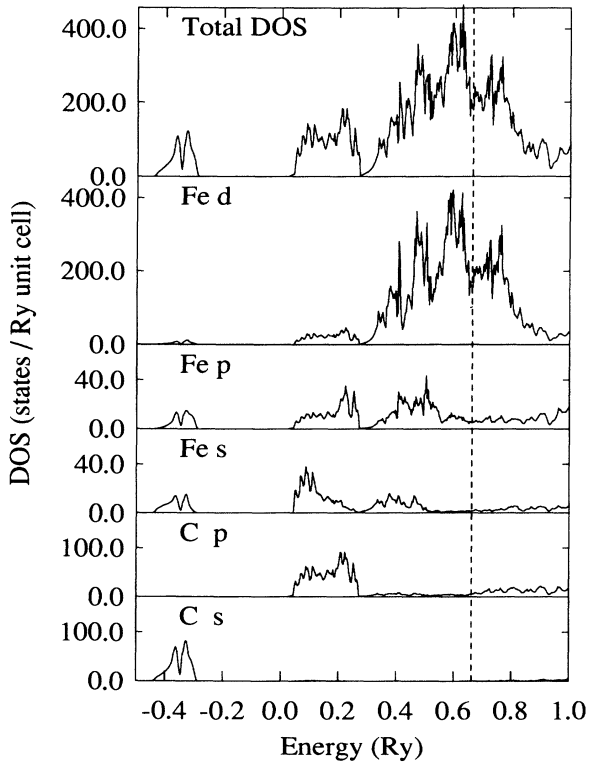

FIG. 3. Density of states curves of Fe_3C. The upper curve shows the total DOS, while *l* projections of iron and carbon atoms are plotted below.

TABLE II. Results from band-structure calculations.

$N(E_F)$ (states/Ry unit cell)		187.8
v_F^2 (cm^2 s^{-2})		0.20×10^{16}
$\hbar\omega_P$ (eV)		5.32
Magnetic moments (μ_B)	Fe(1)	1.98
	Fe(2)	1.74
	C	−0.06
Hyperfine fields (T)	Fe(1)	26.9
	Fe(2)	25.7
	C	0.23
E_{tot} (Ry)		−30 799.3
E_{coh} (mRy/atom)		615

dominate the density of optical phonons. In the case of Fe_3C, this simplification is not possible. In order to get an idea of the size of the electron-phonon coupling in cementite, we set $\langle\omega_{Fe}^2\rangle = \langle\omega_C^2\rangle \approx (k_B\Theta_S/\sqrt{2}\hbar)^2$. Here Θ_S is a Debye temperature from entropy data which, unlike the Debye temperature in the elastic limit, Θ_D, gives considerable weight also to the optical modes. A recent evaluation of thermodynamic data[14] gives $\Theta_S = 394$ K for Fe_3C. We thus obtain $\lambda = 0.77$, which is of the magnitude typical for transition-metal compounds.[19]

The electronic contribution to the heat capacity,

$$\gamma = \tfrac{2}{3}\pi^2 k_B^2 N(E_F)(1+\lambda), \tag{6}$$

becomes $\gamma = 5.4$ mJ/(mol K^2), in reasonable agreement with an experimental[21] value $\gamma = 6.25$ mJ/(mol K^2).

IV. XPS SPECTRA

Spectroscopic investigations of cementite are complicated by the difficulty to obtain a clean Fe_3C surface in an Fe-C system. The carbide phase is experimentally accessible only at the interior of a sample. Outside this region, a layer of iron with chemisorbed[22] carbon is found, while the surface of an Fe-C sample above a certain carbon concentration is covered with graphite. This is why the valence states of Fe_3C could not be probed in ultraviolet photoelectron spectroscopy (UPS) measurements.[22] X-ray photoelectron spectroscopy (XPS) is less sensitive to the surface layers than UPS but it cannot be used to get detailed information on valence states.

The wave functions and the density of states that emerge from band-structure calculations can be used to calculate XPS intensities through the relation[23]

$$I(E_i,\omega) \sim \frac{1}{\omega}\sum_{l_i}\sum_{l_f=l_i\pm1}\frac{\max\{l_i,l_f\}}{(2l_i+1)}N_{l_f}^0(E_i+\hbar\omega) \times N_{l_i}(E_i)|M_{l_f,l_i}(E_i,\omega)|^2, \tag{7}$$

where ω is the x-ray frequency and $N_l(E)$ is the l-projected DOS at energy E. The matrix element M_{l_f,l_i} can be written as an integral over the muffin-tin (MT) sphere,

$$M_{l_f,l_i}(E_i,\omega) = \int_0^S R_{l_f}(E_i+\hbar\omega,r) \times \frac{dV(r)}{dr}R_{l_i}(E_i,r)r^2\,dr, \tag{8}$$

where $R(r)$ is the radial part of the wave function, $V(r)$ is the MT potential, and S is the Wigner-Seitz radius.

The XPS spectrum from the valence bands of Fe_3C has been measured[3] at $T = 653$ K with an Al $K\alpha$ line. It should be noted that this temperature is above the Curie temperature of cementite ($T_C = 488$ K). The comparison with theoretical curves must therefore involve a discussion of the existence of local magnetic ordering in Fe_3C. We return to this question in Sec. VI. In Fig. 4, the experimental XPS intensity from Ref. 3 is plotted on the same energy scale as our theoretical curve, which was obtained as in Eqs. (7) and (8). Because of the high excitation frequency, the density of final states was approximated by $N_{l_f}^0(E+\hbar\omega) \propto 2l+1$. The theoretical and experimental curves in Fig. 4 agree on the positions of the major maxima and minima of the XPS intensity. The experimental curve has maxima at 1.5, 3, 6.5, 8, and 12.5 eV from the vacuum level while maxima in the theoretical intensity occur at 0.9, 2.7, 6.0, 8.9, and 13.5 eV below the Fermi energy. The band-structure calculations in this work confirm the assumptions in Ref. 3 on the origin of the maxima in the XPS intensity of valence levels. The peak e is clearly related to carbon s states. The peaks c and d correspond to the region in the energy spectrum which is important for Fe—C bonds, i.e., where carbon p states are hybridized with iron d states. Finally, the peaks a and b can be associated with Fe—Fe bonds, since they are caused by peaks in the density of unhybridized Fe states.

The XPS intensity in Eq. (7) is a sum over various l_i-l_f transitions. It is then interesting to study which terms in the sum dominate at different energies. The

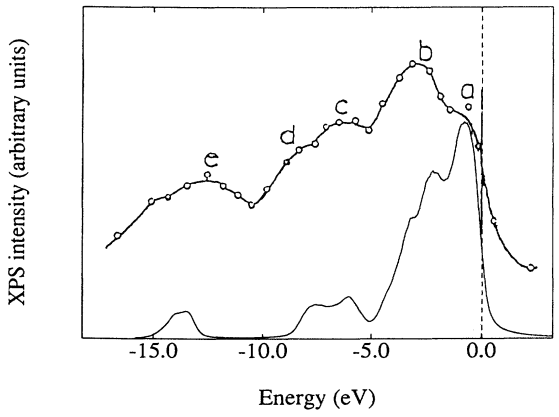

FIG. 4. The theoretical XPS intensity determined in this work (lower curve) plotted vs an experimentally determined intensity from Ref. 3 (upper curve).

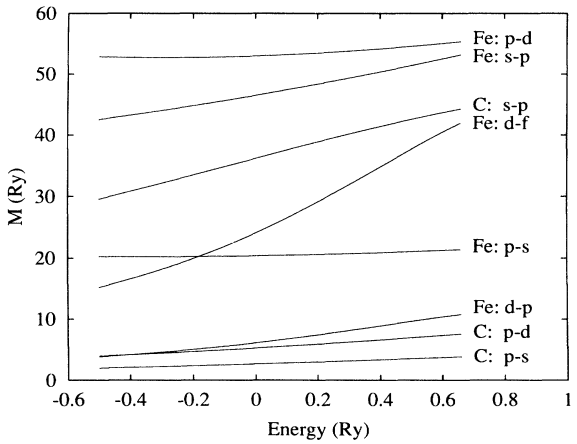

FIG. 5. XPS matrix elements for different l_i-l_f transitions plotted vs the energy.

matrix elements (M_{l_f,l_i}) for the most important transitions are shown in Fig. 5. It is clear that most of these matrix elements remain almost constant over the energy interval corresponding to the valence band. The only important exception is the element belonging to the Fe d-f transition, which increases by a factor of approximately 2.5 over the valence band. This reflects the fact that d functions in transition metals become strongly localized when the energy is close to the Fermi level. Because the muffin-tin potential $V(r)$ has its steepest slope close to the nucleus, this localization effect will increase the XPS matrix element $M_{f,d}$.

V. ELECTRICAL RESISTIVITY

The resistivities for Fe_3C quoted in experimental works are, for various reasons, very uncertain. Radcliffe and Rollason[4] and Masumoto[5] measured the resistivity of two-phase systems containing cementite in a matrix of ferrite and tried to extrapolate to pure cementite. They obtained the resistivities 79.5 and 140 $\mu\Omega$ cm, respectively. Lee and Simkovich[6] recently reported $\rho = 228$ $\mu\Omega$ cm for cementite, but their specimen contained pores. Helsing and Grimvall[24] have reanalyzed the data from Radcliffe and Rollason and from Masumoto, using more accurate descriptions of the effective resistivity of a two-phase mixture. They get $\rho = 104$ and 107 $\mu\Omega$ cm, respectively, for the resistivity of cementite at 300 K.

When $T/\Theta \gtrsim \frac{1}{2}$ the electrical resistivity due to electron-phonon scattering is well approximated by[25]

$$\rho = \left(\frac{2\pi k_B T}{\epsilon_0 \hbar \Omega_{\rm pl}^2}\right) \lambda_{\rm tr}. \tag{9}$$

$\Omega_{\rm pl}$ is the electron plasma frequency and $\lambda_{\rm tr}$ is the dimensionless transport electron-phonon coupling constant. It is usually a good approximation to take $\lambda_{\rm tr} = \lambda$, where λ is the electron-phonon mass enhancement parameter (Sec. III). The Debye temperature of Fe_3C is $\Theta \approx 394$ K,[14] and Eq. (9) should be applicable at ambient temperatures. Following standard procedures,[16–18] we have calculated $\Omega_{\rm pl}$ and λ within the LMTO scheme used here and we get $\lambda = 0.77$, $\hbar\Omega_{\rm pl} = 5.3$ eV. The resulting resistivity is $\rho(298\ {\rm K}) = 31$ $\mu\Omega$ cm. To this value, a magnetic contribution $\rho_{\rm magn}$ should be added. We get a crude estimation of $\rho_{\rm magn}$ from a calculation by Schwerer and Cuddy[26] on pure iron. One can write

$$\rho_{\rm magn} = \rho_0 f(T/T_C). \tag{10}$$

We assume that the temperature dependence of $\rho_{\rm magn}$ is given by the same function $f(T/T_C)$ as for Fe, but with $T_C = 488$ K for Fe_3C. The magnetic moments in Fe_3C are of the same order of magnitude as in Fe, and we let $\rho_0(Fe_3C) \approx \rho_0(Fe)$. Then, for Fe_3C, $\rho_{\rm magn}(298\ {\rm K}) \approx 16$ $\mu\Omega$ cm. Adding this to the contribution from electron-phonon scattering gives $\rho \approx 47$ $\mu\Omega$ cm. Obviously the electron-phonon scattering and the magnetic scattering do not suffice to give a total resistivity as large as suggested by experiments. We believe that the experiments refer to samples with static lattice defects. A large number of such defects might also alter the magnetic behavior, and explain the absence[6] of an anomaly in ρ near $T = T_C$.

VI. DISCUSSION AND CONCLUSION

We have in this paper presented detailed, *ab initio*, LMTO calculations of several electronic properties of Fe_3C (cementite). The overall characteristics of the electronic energy spectrum are similar to those of pure iron or simpler iron carbides. For example, the density of states at the Fermi level is clearly dominated by localized, iron d states. The DOS is high enough for a ferromagnetic spin splitting of the ground state to occur. The magnetic moments determined in our calculations are in excellent agreement with experimental data. The calculated spin densities at the center of each atom have also been used to estimate hyperfine fields, values that also are close to experimental results.

Estimates of the cohesive properties of 3d-transition-metal compounds from *ab initio* band-structure calculations are often in relatively poor agreement with experimental data. This is generally ascribed to shortcomings of the local-density approximation. It is therefore not surprising that our value for the cohesive energy per atom in cementite, $E_{\rm coh} = 615$ mRy, determined as the difference between the total electronic energies of the compound and of its constituent atoms, is somewhat higher than an estimate from experimental information, $E_{\rm coh} = 370$ mRy.[15] However, comparisons between theoretically and experimentally determined cohesive energies in series of simpler transition-metal compounds[11] have shown that the theoretical values can be successfully used to study both general trends and details in the variation of $E_{\rm coh}$, since the shift between theoretical and experimental energies is remarkably constant. It will therefore be interesting to compare our result for the cohesive energy of cementite with results from future investigations of M_3C compounds in the 3d series.

The electronic energy spectrum determined in this work has been used to calculate a theoretical XPS intensity curve in the valence-band region. The comparison with experimental data is complicated by the fact that the only available investigation of the entire valence band refers to a temperature well above the Curie point.[3] There is, however, an overall agreement which lends strong support to our results and which allows for a detailed analysis of the origin of maxima and minima in the intensity. Unfortunately, the experimental resolution is not good enough for any definite conclusion to be drawn as to whether local magnetic moments in Fe_3C persist above the Curie point. There are experimental indications[2] that, unlike in pure fcc iron,[27] the local spin splitting disappears in the paramagnetic state of cementite. Since this transition is not seen in any of the experimental results studied here (e.g., resistivity measurements) we leave this question open.

A question of considerable practical interest concerns the magnitude of the electrical resistivity in Fe_3C. Available measurements give very different results and no theoretical investigation seems to be published. In samples free from defects, one expects that the electrical

resistivity is dominated by the scattering of electrons by phonons. Lacking detailed knowledge of the phonon spectrum of Fe_3C and in absence of sufficient theoretical models for electron-phonon interactions in complex structures, we restrict ourselves to a crude approximation of the vibrational properties of cementite through a high-temperature Debye temperature, Θ_S. The estimated electron-phonon enhancement parameter is $\lambda = 0.77$ and by assuming that this parameter is valid also for transport properties, we get the resistivity $\rho = 41\ \mu\Omega\,\mathrm{m}$. In this estimate, a contribution from the scattering of electrons by magnetic moments has been included. Despite the uncertainty in this resistivity value, one must conclude that experimental investigations refer to samples with a considerable amount of lattice defects.

In conclusion, we have performed the first detailed calculation of the electronic structure of cementite and discussed various physical properties related to the electron states. The experimental data are incomplete or uncertain for several of the properties considered, and our theoretical results add significantly to the information on cementite. This shows how *ab initio* calculations have now reached a stage where they can successfully complement experiments, also for compounds as complex as cementite. We shall exploit this fact in future investigations of other transition-metal compounds.

ACKNOWLEDGMENTS

This work has been supported by the Swedish Natural Science Research Council and by the Swedish Board for Technical Development.

[1] L. J. E. Hofer and E. M. Cohn, J. Am. Chem. Soc. **81**, 1576 (1959).
[2] I. N. Shabanova and V. A. Trapeznikov, Pis'ma Zh. Eksp. Teor. Fiz. **18**, 576 (1973) [JETP Lett. **18**, 339 (1973)].
[3] I. N. Shabanova and V. A. Trapeznikov, J. Electron. Spectrosc. Relat. Phenom. **6**, 297 (1975).
[4] S. V. Radcliffe and E. C. Rollason, J. Iron Steel Inst. **189**, 45 (1958).
[5] H. Masumoto, Sci. Rep. Tohuku Imperial Univ. (Series 1) **16**, 417 (1927).
[6] Ming-Chuan Lee and G. Simkovich, Metall. Trans. **18A**, 485 (1987).
[7] E. J. D. Garba and R. L. Jacobs, J. Phys. Chem. Solids **50**, 101 (1989).
[8] O.K. Andersson, Phys. Rev. B **15**, 3060 (1975).
[9] T. Jarlborg and G. Arbman, J. Phys. F **6**, 189 (1976); **7**, 1635 (1977); G. Arbman and T. Jarlborg, Solid State Commun. **26**, 857 (1978).
[10] R. Wykoff, *Crystal Structures* (Interscience, New York, 1964).
[11] J. Häglund, G. Grimvall, T. Jarlborg, and A. Fernández Guillermet, Phys. Rev. **43**, 14 400 (1991).
[12] W. Y. Ching, Yong-Nian Xu, B. N. Harmon, Jun Ye, and T. C. Leung, Phys. Rev. B **42**, 4460 (1990).
[13] M. Ron and Z. Mathalone, Phys. Rev. B **4**, 774 (1971).
[14] A. Fernández Guillermet and G. Grimvall, J. Phys. Chem. Solids (to be published).
[15] A. Fernández Guillermet (unpublished).
[16] J. C. Phillips, in *Superconductivity in d- and f-band Metals,* edited D. H. Douglass (American Institute of Physics, New York, 1972), p. 339.
[17] G. D. Gaspari and B. L. Gyorffy, Phys. Rev. Lett. **28**, 801 (1972).
[18] M. Dacorogna, T. Jarlborg, A. Junod, M. Pelizzone, and M. Peter, J. Low Temp. Phys. **57**, 629 (1984).
[19] G. Grimvall, *The Electron-Phonon Interaction in Metals* (North-Holland, Amsterdam, 1981).
[20] D. A. Papaconstantopoulous, in *Physics of Transition Metals,* IOP Conf. Proc. No. 55 (Institute of Physics and Physical Society, London, 1980), p. 563; B. M. Klein and D. A. Papaconstantopoulous, Phys. Rev. Lett. **32**, 1193 (1974).
[21] J. Mazur and W. Zacharko, Acta Phys. Pol. **35**, 91 (1969).
[22] G. Panzner and W. Diekmann, Surf. Sci. **160**, 253 (1985).
[23] T. Jarlborg and P. O. Nilsson, J. Phys. C **12**, 265 (1979).
[24] J. Helsing and G. Grimvall, J. Appl. Phys. (to be published).
[25] P. B. Allen, Phys. Rev. B **36**, 2920 (1987).
[26] F. C. Schwerer and L. J. Cuddy, Phys. Rev. B **2**, 1575 (1970).
[27] V. Heine, A. I. Liechtenstein, and O. N. Mryasov, Europhys. Lett. **12**, 545 (1990).